

# Position/force control of uncertain constrained flexible joint robots

L. Huang<sup>a,\*</sup>, S.S. Ge<sup>b</sup>, T.H. Lee<sup>b</sup>

<sup>a</sup> School of Electrical and Electronics Engineering, Singapore Polytechnic, Singapore 139651, Singapore

<sup>b</sup> Department of Electrical and Computer Engineering, National University of Singapore, Singapore 117576, Singapore

Received 9 March 2004; accepted 28 October 2005

## Abstract

This paper addresses the issue of adaptive position/force control of uncertain constrained flexible joint robots (FJR). The controller is developed without the assumptions of weak robot joint flexibility as adopted in popular singular perturbation (SP) approaches. It relies on the feedback of joint state variables and avoids noisy joint torque measurements found in most controllers developed so far. In addition to the robot inertia parameters, the joint stiffness and the motor inertia are also assumed to be unknown. The proposed approach achieves the position tracking and the boundedness of force errors. The simulation study is conducted to verify the effectiveness of the approach.

© 2005 Elsevier Ltd. All rights reserved.

**Keywords:** Constrained robots; Position/force control; Flexible joint robots

## 1. Introduction

Control of flexible joint robotic manipulators has been studied extensively in the last decades, almost parallel to that of rigid joint robotic manipulators. With singular perturbation (SP) analysis, controllers developed for rigid robotic manipulators, adaptive or non-adaptive, can be readily extended for the robots of *weak* joint flexibilities (the joint stiffness is very big) [1–6]. Feedback linearization method was also used in the controller design, but it required exact dynamic modeling of the robot and the measurements of its joint accelerations and jerks [7,8]. To deal with the uncertainties of robotic systems, many adaptive control schemes [9–11] were developed from the pioneering work on adaptive control of rigid robotic manipulators in [12]. To cope with the complexity of the system dynamics, the controller design required joint acceleration feedback, filtering of system dynamics and the calculation of the inverse inertia matrix of the robot. The controller was com-

plex in structure and computationally intensive. Treating a flexible joint robotic manipulator as a cascading system, joint torque feedback and backstepping approaches were also applied in the controller design [13,14]. They required the measurement of joint torques and their derivatives which are normally very noisy.

Compared with those of free flexible joint robots, fewer research results were reported on controlling constrained flexible joint robotic manipulators. The challenge for controlling an uncertain constrained robot with arbitrary flexibility lies in the constraint force term which is in an algebraic relation to the system dynamics and is difficult to be handled in controller synthesis and stability analysis. Most researches focused on the robot systems with *known* parameters and *weak* joint flexibility [15,16]. In [17], a Cartesian-space robot model were used to develop the position control and the force control along certain curvilinear directions as proposed in [18]. The joint torque and its up to second-order derivatives are required in the controller design. In [19], a Cartesian impedance control of flexible joint robots was developed based on joint torque feedback. With computed torque control, the joint dynamics and the link dynamics were decoupled and the desired impedance

\* Corresponding author. Tel.: +65 68790663; fax: +65 67721974.  
E-mail address: [loulin@sp.edu.sg](mailto:loulin@sp.edu.sg) (L. Huang).

was achieved. It needed an exact knowledge of the system dynamics and the noisy joint torque feedback.

In this paper, an adaptive position/force controller is developed for an uncertain constrained robot with flexible joints. It mainly relies on the feedbacks of *joint state variables* (joint positions and velocities) and thus avoids noisy joint torque feedback. The joint stiffness and the motor inertia are also assumed to be unknown in addition to the robot inertia parameters which were normally assumed to be known in most controllers developed so far. The controller is designed with a Lyapunov-based cascaded approach. In the first step, a desired joint position is found to make a Lyapunov function of link position tracking error and the constraint force error non-increasing. In the second step, the control input is derived to make the joint position to track its trajectory obtained in the first step. As the joint torque feedback is not used in the controller, the joint stiffness becomes an uncertain parameter scaling the control input of a subsystem of the whole controlled system. This additional challenge to the controller design was overcome with the results reported in [20]. The proposed approach achieves the position tracking and the boundedness of force errors. The simulation study is conducted to verify the effectiveness of the approach.

The paper is organized as follows. In Section 2, the system dynamics and problem formulation is described. In Section 3, the controller design and its stability analysis are provided. Section 4 presents the simulation results to verify the effectiveness of the controller. The conclusion is given in Section 5.

## 2. Dynamical model and properties

Consider the dynamic model of a constrained flexible joint robot as proposed in [15],

$$M(q_l)\ddot{q}_l + C(q_l, \dot{q}_l)\dot{q}_l + G(q_l) = K_s\theta + f, \quad (1)$$

$$J_m\ddot{q}_m + K_s\theta = \tau_m, \quad (2)$$

$$\theta \triangleq q_m - q_l, \quad (3)$$

where  $q_l \in R^n$  and  $q_m \in R^n$  are the positions of the robot links and the motor shafts, respectively,  $M(q_l) \in R^{n \times n}$  is the inertia matrix of rigid links,  $C(q_l, \dot{q}_l)$  is the Coriolis and centrifugal force matrix,  $G(q_l)$  is the gravitational force,  $J_m = \text{diag}[j_{mi}] \in R^{n \times n}$  is the positive definite diagonal matrix of the moments of inertia of the motors,  $K_s = \text{diag}[k_{si}] \in R^{n \times n}$  is the positive definite diagonal matrix of the joint stiffness,  $f \in R^n$  is the joint torque contributed by the constraint force and  $\tau_m \in R^n$  is the input torque of the motors.  $j_{mi}$  and  $k_{si}$  ( $i = 1, 2, \dots, n$ ) are the inertia and the stiffness of  $i$ th joint.  $n$  is the degree of freedom of the robotic manipulator.

Assuming that the holonomic and frictionless constraint surface is described by

$$\Phi(q_l) = 0 \in R^m, \quad (4)$$

where  $\Phi(q_l)$  is a set of independent equations and are twice continuously differentiable [21].

Constraint force in the joint space,  $f$ , can then be expressed by

$$f = J^T(q_l)\lambda, \quad (5)$$

$$J(q_l) \triangleq \frac{\partial \Phi(q_l)}{\partial q_l} \in R^{m \times n},$$

where  $\lambda \in R^m$  is a generalized Lagrange multiplier relating to the magnitude of the constraint force [21].  $m$  is the dimension of the constraint surface and it is assumed that  $m < n$ .

Due to the  $m$ -dimension constraint,  $m$  degrees of freedom of the robot are lost. Partitioning the link position vector  $q_l$  to  $q_l^1 \in R^{n-m}$  and  $q_l^2 \in R^m$ , we have

$$q_l = [q_l^{1T} \quad q_l^{2T}]^T \quad (6)$$

and accordingly, the Jacobian  $J(q_l)$  is decomposed as

$$J(q_l) = [J_1(q_l) \quad J_2(q_l)], \quad (7)$$

$$J_1(q_l) \triangleq \frac{\partial \Phi(q_l)}{\partial q_l^1} \in R^{m \times (n-m)},$$

$$J_2(q_l) \triangleq \frac{\partial \Phi(q_l)}{\partial q_l^2} \in R^{m \times m}.$$

As stated in [22], it is possible to have a partition such that  $J_2^{-1}(q_l)$  exists and

$$\dot{q}_l = L(q_l)\dot{q}_l^1, \quad L(q) = \begin{bmatrix} I_{n-m} \\ -J_2^{-1}(q_l)J_1(q_l) \end{bmatrix}, \quad (8)$$

where  $I_{n-m}$  is an identity matrix of dimension  $n - m$ .

With the partition of the link position vector in Eq. (6), the position of the robot can be uniquely determined by  $q_l^1$ . The original dynamical model in Eqs. (1) and (2) is transformed to

$$M^1(q_l)\ddot{q}_l^1 + C^1(q_l, \dot{q}_l)\dot{q}_l^1 + G^1(q_l) = K_s\theta + J^T(q_l)\lambda, \quad (9)$$

$$J_m\ddot{q}_m + K_s\theta = \tau_m, \quad (10)$$

where

$$M^1(q_l) = M(q_l)L(q_l) \in R^{(n-m) \times (n-m)},$$

$$C^1(q_l, \dot{q}_l) = M(q_l)\dot{L}(q_l) + C(q_l, \dot{q}_l)L(q_l) \in R^{(n-m) \times (n-m)},$$

$$G^1(q_l) = G(q_l) \in R^{n-m}.$$

Define  $M_\lambda(q_l) = L^T(q_l)M^1(q_l) \in R^{m \times m}$ ,  $C_\lambda(q_l, \dot{q}_l) = L^T(q_l) \times C^1(q_l, \dot{q}_l) \in R^{m \times m}$  and  $G_\lambda(q_l) = L^T(q_l)G^1(q_l) \in R^m$ . It can be proved that the dynamic models (1) and (9) have the following properties.

**Property 1.**  $L^T(q_l)J^T(q_l) = 0$ .

**Property 2.**  $M(q_l)$ ,  $C(q_l, \dot{q}_l)$ ,  $G(q_l)$ ,  $M^1(q_l)$ ,  $C^1(q_l, \dot{q}_l)$ ,  $G^1(q_l)$ ,  $M_\lambda(q_l)$ ,  $C_\lambda(q_l, \dot{q}_l)$ ,  $G_\lambda(q_l)$ ,  $L(q_l)\dot{L}(q_l)$ , and  $J(q_l)$  are uniformly bounded and continuous if  $q_l$  and  $\dot{q}_l$  are uniformly bounded and continuous;  $M(q_l)$  and  $M_\lambda(q_l)$  are symmetric positive definite (s.p.d.).

**Property 3.**  $\dot{M}(q_1) - 2C(q_1, \dot{q}_1)$  and  $\dot{M}_L(q_1) - 2C_L(q_1, \dot{q}_1)$  are skew-symmetric if  $C(q_1, \dot{q}_1)$  is in the Christoffel form, i.e.,  $x_1^T(\dot{M}(q_1) - 2C(q_1, \dot{q}_1))x_1 = 0$ ,  $x_2^T(\dot{M}_L(q_1) - 2C_L(q_1, \dot{q}_1))x_2 = 0$ ,  $\forall x_1 \in R^n$  and  $x_2 \in R^{n-m}$ .

**Property 4.** The robot link dynamics described by Eq. (1) is linear in the robot link parameters, i.e., given an arbitrary vector  $x \in R^n$

$$M(q_1)\dot{x} + C(q_1, \dot{q}_1)x + G(q_1) = \Psi(\dot{x}, x, \dot{q}_1, q_1)p, \quad (11)$$

where  $p \in R^l$  is a vector of the lumped parameters of interest,  $\Psi(\dot{x}, x, \dot{q}_1, q_1) \in R^{n \times l}$  is a regressor matrix.

If the estimates of  $M(q_1)$ ,  $C(q_1, \dot{q}_1)$  and  $G(q_1)$  are denoted by  $\hat{M}(q_1)$ ,  $\hat{C}(q_1, \dot{q}_1)$  and  $\hat{G}(q_1)$ , then

$$\hat{M}(q_1)\dot{x} + \hat{C}(q_1, \dot{q}_1)x + \hat{G}(q_1) = \Psi(\dot{x}, x, \dot{q}_1, q_1)\hat{p}, \quad (12)$$

where  $\hat{p}$  is the estimate of  $p$ .

**Property 5** [20]. If the regressor matrix  $\Psi(\dot{x}, x, \dot{q}_1, q_1)$  and the vector  $p$  in Eq. (11) are given in the following forms:

$$\Psi(\dot{x}, x, \dot{q}_1, q_1) = \begin{bmatrix} \psi_1^T(\dot{x}, x, \dot{q}_1, q_1) & 0 & \cdots & 0 \\ 0 & \psi_2^T(\dot{x}, x, \dot{q}_1, q_1) & \cdots & 0 \\ \cdots & \cdots & \cdots & \cdots \\ 0 & 0 & \cdots & \psi_n^T(\dot{x}, x, \dot{q}_1, q_1) \end{bmatrix} \in R^{n \times l}, \quad (13)$$

$$p = [p_1^T \ p_2^T \ \cdots \ p_n^T]^T \in R^l, \quad (14)$$

then

$$K_s \Psi(\dot{x}, x, \dot{q}_1, q_1)p = \Psi(\dot{x}, x, \dot{q}_1, q_1)p_s,$$

where

$$p_s \triangleq [k_{s1}p_1^T \ k_{s2}p_2^T \ \cdots \ k_{sn}p_n^T]^T = Ap \in R^l,$$

$$A \triangleq \begin{bmatrix} \text{diag}[k_{s1}] & 0 & \cdots & 0 \\ 0 & \text{diag}[k_{s2}] & \cdots & 0 \\ \cdots & \cdots & \cdots & \cdots \\ 0 & 0 & \cdots & \text{diag}[k_{sn}] \end{bmatrix} \in R^{l \times l}$$

and  $\psi_l(\dot{x}, x, \dot{q}_1, q_1) \in R^{n_l}$ ,  $p_l \in R^{n_l}$ ,  $\text{diag}[k_{sl}] \in R^{n_l \times n_l}$ ,  $l = \sum_{i=1}^n n_i$ ,  $i = 1, 2, \dots, n$ .

Assume that  $K_s$  and  $J_m$  are unknown and their estimates are denoted as  $\hat{K}_s$ , and  $\hat{J}_m$ , respectively. Their estimate errors are defined as  $\tilde{K}_s \triangleq K_s - \hat{K}_s$  and  $\tilde{J}_m \triangleq J_m - \hat{J}_m$ , respectively. For the controller design, the following assumptions are made for these terms.

**Assumption 1.**  $K_s$  and  $J_m$  are unknown and bounded.

**Assumption 2.**  $\tilde{K}_s$  and  $\tilde{J}_m$  are bounded such that  $\|\tilde{K}_s\| \leq \delta_K$  and  $\|\tilde{J}_m\| \leq \delta_J$ , where  $\delta_K$  and  $\delta_J$  are known positive constants.

**Assumption 3.**  $q_l(t)$ ,  $q_m(t)$ ,  $\dot{q}_l(t)$ ,  $\dot{q}_m(t)$ ,  $\ddot{q}_m$  and  $\lambda(t)$  are all measurable.

Barbalat's lemma is important to the controller design and analysis [23,25]. It is listed below for an easy reference.

**Lemma 1** (Barbalat). If the differentiable function  $f(t)$  has a finite limit as  $t \rightarrow \infty$ , and if  $\dot{f}$  is uniformly continuous, then  $\dot{f} \rightarrow 0$  as  $t \rightarrow \infty$ .

As the boundedness of  $\dot{f}$  is a sufficient condition of uniform continuity of  $f$ , a practical corollary of Barbalat's lemma can be stated as

**Corollary 1** (Barbalat). If the differentiable function  $f(t)$  has a finite limit as  $t \rightarrow \infty$ , and is such that  $\dot{f}$  exists and is bounded, then  $\dot{f} \rightarrow 0$  as  $t \rightarrow \infty$ .

### 3. Controller design

Let  $q_{ld}(t)$  be the desired trajectory of the link position and  $\lambda_d(t)$  be the desired magnitude of the constraint force. The control objective is to find a driving torque  $\tau_m$  under which  $q(t)$  tracks  $q_{ld}(t)$  and the error between  $\lambda(t)$  and  $\lambda_d(t)$  is bounded. It is only necessary to make  $q_l^1(t)$  track its desired trajectory  $q_{ld}^1(t)$  since  $q_l^1(t)$  completely determines  $q(t)$ .

From dynamic model represented by Eqs. (9) and (10), a cascaded Lyapunov based control design approach can be adopted to derive the control input  $\tau_m$ . In the first step, a desired value of  $\theta$ :  $\theta_d$ , is determined aiming at making  $q_l^1(t)$  track  $q_{ld}^1(t)$  and the boundedness of  $\lambda_d(t) - \lambda(t)$ . Then, the control input  $\tau_m$  is obtained to make  $\theta$  to track  $\theta_d$ .

Define the following variables which are related to the tracking errors of the link position and the constraint force:

$$e^1 \triangleq q_{ld}^1 - q_l^1, \quad e_\lambda \triangleq \lambda_d - \lambda, \quad (15)$$

$$r^1 \triangleq \dot{e}^1 + K_e e^1, \quad \dot{q}_r^1 \triangleq \dot{q}_{ld}^1 + K_e e^1, \quad (16)$$

where  $K_e \in R^{(n-m) \times (n-m)}$  is a positive definite constant matrix.

With variables  $r^1$  and  $q_r^1$ , the following variables are also defined:

$$\sigma \triangleq L(q_l)r^1 + \mu, \quad (17)$$

$$v \triangleq L(q_l)\dot{q}_r^1 + \mu, \quad (18)$$

where  $\mu$  is a variable introduced to compensate the force error  $e_\lambda$  and it will be determined later.

From Eqs. (17) and (18), it is obvious that

$$r^1 = \dot{q}_r^1 - \dot{q}_l^1, \quad (19)$$

$$\sigma = v - L(q_l)\dot{q}_l^1, \quad (20)$$

$$\dot{\sigma} = \dot{v} - L(q_l)\ddot{q}_l^1 - \dot{L}(q_l)\dot{q}_l^1. \quad (21)$$

For the parameters update, the following vectors are constructed with the elements of diagonal matrices  $K_s$ ,  $\hat{K}_s$  and  $\tilde{K}_s^{-1}$ .

$$k_s^{-1} \triangleq [k_{s1}^{-1} \ k_{s2}^{-1} \ \cdots \ k_{sn}^{-1}]^T, \quad (22)$$

$$\hat{k}_s^{-1} \triangleq [\hat{k}_{s1}^{-1} \ \hat{k}_{s2}^{-1} \ \cdots \ \hat{k}_{sn}^{-1}]^T, \quad (23)$$

$$\tilde{k}_s^{-1} = k_s^{-1} - \hat{k}_s^{-1}, \quad (24)$$

$$\varphi_1(K_s, \hat{K}_s^{-1}) \triangleq K_s \hat{k}_s^{-1} = [k_{s1} \tilde{k}_{s1}^{-1} \ k_{s2} \tilde{k}_{s2}^{-1} \ \cdots \ k_{sn} \tilde{k}_{sn}^{-1}]^T, \quad (25)$$

where  $k_{si}$  is the stiffness of  $i$ th joint and  $\hat{k}_{si}^{-1}$  is the estimate of  $k_{si}^{-1}$ .

Note that  $\hat{K}_s^{-1}$  and  $\hat{k}_s^{-1}$  here only serve as the estimates of  $K_s^{-1}$  and  $k_s^{-1}$ , respectively. They are NOT the inverses of  $\hat{K}_s$  and  $\hat{k}_s$ , respectively.

### 3.1. Step 1. Determination of $\theta_d$ : the desired value of $\theta$

In this step,  $\theta_d$ , the desired value of  $\theta$ , is determined to make a Lyapunov function of  $e_1$ ,  $e_\lambda$  and the system parameter estimation errors non-increasing.

Consider the following Lyapunov function:

$$V_1 = \frac{1}{2} \sigma^T M(q_l) \sigma + \frac{1}{2} (p - \hat{p}_s)^T \Gamma_1 (p - \hat{p}_s) + \frac{1}{2} \mu^T \mu + \frac{1}{2} \phi_1^T(K_s, \hat{K}_s^{-1}) \Gamma_2 \phi_1(K_s, \hat{K}_s^{-1}),$$

where  $\hat{p}_s$  is the estimate of  $p_s$  as defined in Property 5,  $\Gamma_1 \in R^{k \times k}$  and  $\Gamma_2 \in R^{n \times n}$  are positive definite diagonal matrices. Note that  $p - \hat{p}_s$ , instead of  $p - \hat{p}$ , is used in the above definition so that the unknown joint stiffness  $K_s$  lumped in  $p_s$  is also taken care of by the controller to be developed.

Differentiating  $V_1$  with respect to time  $t$  and considering Properties 3 and 5, we have

$$\begin{aligned} \dot{V}_1 &= \sigma^T M(q_l) \dot{\sigma} + \frac{1}{2} \sigma^T \dot{M}(q_l) \sigma - (p - \hat{p}_s)^T \Gamma_1 \dot{\hat{p}}_s \\ &\quad + \mu^T \dot{\mu} + \phi_1^T(K_s, \hat{K}_s^{-1}) \Gamma_2 \dot{\phi}_1(K_s, \hat{K}_s^{-1}) \\ &= \sigma^T (M(q_l) \dot{\sigma} + C(q_l, \dot{q}_l) \sigma) - (p - \hat{p}_s)^T \Gamma_1 \dot{\hat{p}}_s + \mu^T \dot{\mu} \\ &\quad + \phi_1^T(K_s, \hat{K}_s^{-1}) \Gamma_2 \dot{\phi}_1(K_s, \hat{K}_s^{-1}). \end{aligned} \quad (26)$$

Substituting  $\sigma$  in Eq. (20) and  $\dot{\sigma}$  in Eq. (21) into Eq. (26), we have

$$\begin{aligned} \dot{V}_1 &= \sigma^T (M(q_l) \dot{v} + C(q_l, \dot{q}_l) v + G(q_l) - M^1(q_l) \ddot{q}_l^1 \\ &\quad - C^1(q_l, \dot{q}_l) \dot{q}_l^1 - G^1(q_l)), -(p - \hat{p}_s)^T \Gamma_1 \dot{\hat{p}}_s + \mu^T \dot{\mu} \\ &\quad + \phi_1^T(K_s, \hat{K}_s^{-1}) \Gamma_2 \dot{\phi}_1(K_s, \hat{K}_s^{-1}). \end{aligned} \quad (27)$$

Considering Eq. (9) and Property 4, Eq. (27) leads to

$$\begin{aligned} \dot{V}_1 &= \sigma^T (\Psi(\dot{v}, v, \dot{q}_l, q_l) p - K_s \theta - J^T(q_l) \lambda) - (p - \hat{p}_s)^T \Gamma_1 \dot{\hat{p}}_s \\ &\quad + \mu^T \dot{\mu} + \phi_1^T(K_s, \hat{K}_s^{-1}) \Gamma_2 \dot{\phi}_1(K_s, \hat{K}_s^{-1}). \end{aligned} \quad (28)$$

Our aim is to find  $\theta_d$ , the desired value of  $\theta$  to make  $\dot{V}_1$  non-positive. Define the difference between  $\theta$  and  $\theta_d$  as

$$z \triangleq \theta_d - \theta$$

and Eq. (28) can be re-written as

$$\begin{aligned} \dot{V}_1 &= \sigma^T (\Psi(\dot{v}, v, \dot{q}_l, q_l) p - K_s \theta_d - J^T(q_l) \lambda) - (p - \hat{p}_s)^T \Gamma_1 \dot{\hat{p}}_s \\ &\quad + \mu^T \dot{\mu} + \phi_1^T(K_s, \hat{K}_s^{-1}) \Gamma_2 \dot{\phi}_1(K_s, \hat{K}_s^{-1}) + \sigma^T K_s z. \end{aligned} \quad (29)$$

Letting

$$\theta_d = K_s \sigma - \hat{K}_s^{-1} J^T(q_l) \lambda_d + \Psi(\dot{v}, v, \dot{q}_l, q_l) \hat{p}, \quad (30)$$

where  $K_s \in R^{n \times n}$  is positive definite and  $\hat{p}$  is the estimate of  $p$ , and substituting it into Eq. (29), we have

$$\begin{aligned} \dot{V}_1 &= \sigma^T (\Psi(\dot{v}, v, \dot{q}_l, q_l) p - K_s \Psi(\dot{v}, v, \dot{q}_l, q_l) \hat{p}) \\ &\quad - \sigma^T K_s K_s \sigma + \sigma^T K_s \hat{K}_s^{-1} J^T(q_l) \lambda_d - \sigma^T J^T(q_l) \lambda \\ &\quad - (p - \hat{p}_s)^T \Gamma_1 \dot{\hat{p}}_s + \mu^T \dot{\mu} \\ &\quad + \phi_1^T(K_s, \hat{K}_s^{-1}) \Gamma_2 \dot{\phi}_1(K_s, \hat{K}_s^{-1}) + \sigma^T K_s z. \end{aligned} \quad (31)$$

From the definition of  $\sigma$  in Eq. (17) and Property 1, it is obvious that

$$\begin{aligned} \sigma^T J^T(q_l) \lambda &= \mu^T J^T(q_l) \lambda, \\ \sigma^T K_s \hat{K}_s^{-1} J^T(q_l) \lambda_d &= \mu^T J^T(q_l) \lambda_d - \sigma^T K_s \tilde{K}_s^{-1} J^T(q_l) \lambda_d. \end{aligned}$$

Substituting the above terms into Eq. (31) and considering Property 5, we have

$$\begin{aligned} \dot{V}_1 &= (p - \hat{p}_s)^T (\Psi^T(\dot{v}, v, \dot{q}_l, q_l) \sigma - \Gamma_1 \dot{\hat{p}}_s) - \sigma^T K_s K_s \sigma \\ &\quad + \mu^T J^T(q_l) e_\lambda - \sigma^T K_s \tilde{K}_s^{-1} J^T(q_l) \lambda_d + \mu^T \dot{\mu} \\ &\quad + \phi_1^T(K_s, \hat{K}_s^{-1}) \Gamma_2 \dot{\phi}_1(K_s, \hat{K}_s^{-1}) + \sigma^T K_s z. \end{aligned} \quad (32)$$

Letting  $\mu$  evolves according to

$$\dot{\mu} + K_\mu \mu = -J^T(q_l) e_\lambda, \quad (33)$$

where  $K_\mu \in R^{n \times n}$  is a positive definite constant matrix, and substituting it into Eq. (32), we have

$$\begin{aligned} \dot{V}_1 &= (p - \hat{p}_s)^T (\Psi^T(\dot{v}, v, \dot{q}_l, q_l) \sigma - \Gamma_1 \dot{\hat{p}}_s) \\ &\quad - \sigma^T K_s \tilde{K}_s^{-1} J^T(q_l) \lambda_d - \sigma^T K_s K_s \sigma - \mu^T K_\mu \mu \\ &\quad + \phi_1^T(K_s, \hat{K}_s^{-1}) \Gamma_2 \dot{\phi}_1(K_s, \hat{K}_s^{-1}) + \sigma^T K_s z. \end{aligned} \quad (34)$$

As both  $K_s$  and  $\tilde{K}_s^{-1}$  are diagonal matrices, it is easy to verify that

$$\sigma^T K_s \tilde{K}_s^{-1} J^T(q_l) \lambda_d = \phi_1^T(K_s, \hat{K}_s^{-1}) \phi_2(\sigma, q_l, \lambda_d), \quad (35)$$

where

$$\phi_2(\sigma, q_l, \lambda_d) \triangleq [(J^T(q_l) \lambda_d)_1 \sigma_1 (J^T(q_l) \lambda_d)_2 \sigma_2 \cdots (J^T(q_l) \lambda_d)_n \sigma_n]^T \quad (36)$$

and  $(J^T(q_l) \lambda_d)_i$  and  $\sigma_i$  are the  $i$ th elements of  $J^T(q_l) \lambda_d$  and  $\sigma$ , respectively. The vector  $\phi_1(K_s, \hat{K}_s^{-1})$  is already defined in Eq. (25).

Substituting Eq. (35) into Eq. (34), we have

$$\begin{aligned} \dot{V}_1 &= (p - \hat{p}_s)^T (\Psi^T(\dot{v}, v, \dot{q}_l, q_l) \sigma - \Gamma_1 \dot{\hat{p}}_s) \\ &\quad - \phi_1^T(K_s, \hat{K}_s^{-1}) (\phi_2(\sigma, q_l, \lambda_d) - \Gamma_2 \dot{\phi}_1(K_s, \hat{K}_s^{-1})) \\ &\quad + \sigma^T K_s z - \mu^T K_\mu \mu - \sigma^T K_s K_s \sigma. \end{aligned} \quad (37)$$

Letting

$$\dot{\hat{p}}_s = \Gamma_1^{-1} \Psi^T(\dot{v}, v, \dot{q}_l, q_l) \sigma \quad (38)$$

$$\phi_1(K_s, \hat{K}_s^{-1}) = \Gamma_2^{-1} \phi_2(\sigma, q_l, \lambda_d) \quad (39)$$

and substituting them into Eq. (37), it follows that

$$\dot{V}_1 = \sigma^T K_s z - \mu^T K_\mu \mu - \sigma^T K_s K_\sigma \sigma. \quad (40)$$

As  $K_\mu$  and  $K_s K_\sigma$  are all positive definite, it follows that

$$\dot{V}_1 \leq \sigma^T K_s z \quad (41)$$

and when  $z = 0$ , that is,  $\theta = \theta_d$ ,  $\dot{V}_1 \leq 0$ .

From Eq. (38) and the definition of  $p_s$  in Property 5, we have

$$\dot{p} = \Gamma_p \Psi^T(\dot{v}, v, \dot{q}_l, q_l) \sigma, \quad (42)$$

where  $\Gamma_p \triangleq A^{-1} \Gamma_1^{-1}$ .

From Eq. (39) and the definition of  $\varphi_1(K_s, \hat{K}_s^{-1})$  in Eq. (25), we have

$$\dot{k}_s^{-1} = -\Gamma_k \varphi_2(\sigma, q_l, \lambda_d), \quad (43)$$

where  $\Gamma_k \triangleq K_s^{-1} \Gamma_2^{-1}$ .

Once the elements of  $\hat{k}_s^{-1}$  are determined through adaptation law in Eq. (43), they are then used to form the diagonal matrix  $\hat{K}_s^{-1}$  needed for the calculation of  $\theta_d$  in Eq. (30).

**Remark 1.** The uncertain terms  $A$  and  $K_s$  are ‘‘lumped’’ in the parameter adaptation gains  $\Gamma_p$  and  $\Gamma_k$ , respectively.  $\Gamma_p$  and  $\Gamma_k$  are always positive definite due to the fact that  $A$ ,  $K_s$ ,  $\Gamma_1$  and  $\Gamma_2$  are positive definite, and this meets the requirement for parameter adaptation.

### 3.2. Step 2. Determination of input torque: $\tau_m$

In this step, the control input  $\tau_m$  will be derived to make a Lyapunov function of  $z$ ,  $e^1$  and  $e_\lambda$  non-increasing.

Defining a Lyapunov function

$$\begin{aligned} V_2 &= V_1 + \frac{1}{2} z^T K_s z \\ &= \frac{1}{2} \sigma^T M(q_l) \sigma + \frac{1}{2} (p - \hat{p}_s)^T \Gamma_1 (p - \hat{p}_s) + \frac{1}{2} \mu^T \mu \\ &\quad + \varphi_1^T(K_s, \hat{K}_s^{-1}) \Gamma_2 \varphi_1(K_s, \hat{K}_s^{-1}) + \frac{1}{2} z^T K_s z \end{aligned} \quad (44)$$

and differentiating it with respect to time  $t$ , we have

$$\dot{V}_2 = \dot{V}_1 + \dot{z}^T K_s z. \quad (45)$$

Obviously,  $V_2$  as well as  $V_1$  is continuous, positive definite and radially unbounded.

With  $\theta_d$  given in Eq. (30),  $\hat{p}$  and  $\hat{k}_s^{-1}$  adaptively tuned in Eqs. (42) and (43), respectively, it has been shown that

$$\dot{V}_1 = \sigma^T K_s z - \mu^T K_\mu \mu - \sigma^T K_s K_\sigma \sigma \quad (46)$$

and, as a result,

$$\begin{aligned} \dot{V}_2 &= (\sigma + \dot{z})^T K_s z - \mu^T K_\mu \mu - \sigma^T K_s K_\sigma \sigma \\ &= (\sigma + \dot{z})^T (K_s \theta_d - K_s \theta) - \mu^T K_\mu \mu - \sigma^T K_s K_\sigma \sigma. \end{aligned} \quad (47)$$

Solving  $K_s \theta$  in Eq. (2) and substituting it into Eq. (47), we have

$$\dot{V}_2 = (\sigma + \dot{z})^T (K_s \theta_d - \tau_m + J_m \ddot{q}_m) - \mu^T K_\mu \mu - \sigma^T K_s K_\sigma \sigma. \quad (48)$$

Letting

$$\tau_m = \hat{K}_s \theta_d + \hat{J}_m \ddot{q}_m + k_\tau \text{sgn}(\sigma + \dot{z}), \quad (49)$$

$$k_\tau \geq \delta_K \|\theta_d\| + \delta_J \|\ddot{q}_m\|, \quad (50)$$

where  $\hat{K}_s$  and  $\hat{J}_m$  are the estimates of  $K_s$  and  $J_m$ , respectively, as defined in Assumption 1, and,  $\delta_K$  and  $\delta_J$  are the bounds of  $\tilde{K}_s$  and  $\tilde{J}_m$ , respectively, as defined in Assumption 2.  $\text{sgn}(\sigma + \dot{z})$  is a sign function applying on  $\sigma + \dot{z}$  element wise such that 1 is returned when an element of  $\sigma + \dot{z}$  is non-negative or  $-1$  otherwise.

Substituting  $\tau_m$  into Eq. (48), it turns out that

$$\begin{aligned} \dot{V}_2 &= (\sigma + \dot{z})^T (\tilde{K}_s \theta_d + \tilde{J}_m \ddot{q}_m - k_\tau \text{sgn}(\sigma + \dot{z})) - \mu^T K_\mu \mu \\ &\quad - \sigma^T K_s K_\sigma \sigma. \end{aligned} \quad (51)$$

Noting the definition of  $k_\tau$ , we have

$$(\sigma + \dot{z})^T (\tilde{K}_s \theta_d + \tilde{J}_m \ddot{q}_m - k_\tau \text{sgn}(\sigma + \dot{z})) \leq 0 \quad (52)$$

and thus

$$\dot{V}_2 \leq -\mu^T K_\mu \mu - \sigma^T K_s K_\sigma \sigma \leq 0. \quad (53)$$

From here, we are ready to study the boundedness and the convergence of the closed-loop signals.

As  $\dot{V}_2 \leq 0$  and  $V_2$  is non-increasing, this guarantees the boundedness of  $\sigma$ ,  $p - \hat{p}_s$ ,  $\mu$ ,  $\varphi_1(K_s, \hat{K}_s^{-1})$  and  $z$ , consequently,  $v$ ,  $\varphi_2(\sigma, q_l, \lambda_d)$  and  $r^1$  are also bounded from the definition. This means that all of the signals of the closed-loop system are bounded on  $[0, t_f]$  where  $t_f$  defines the maximum time interval for the existence of these signals. It is obvious that the boundedness of the signals is independent of  $t_f$ , and thus all the closed loop signals are globally uniformly bounded on  $[0, \infty]$ .

To analyze the force response, first  $\Psi(\dot{v}, v, \dot{q}_l, q_l) \dot{p}$  is expanded from Property 4,

$$\Psi(\dot{v}, v, \dot{q}_l, q_l) \dot{p} = \hat{M}(q_l) \dot{v} + \hat{C}(q_l, \dot{q}_l) v + \hat{G}(q_l). \quad (54)$$

Substituting  $v$  defined in Eq. (18) into Eq. (54) and considering Eq. (33), we have

$$\begin{aligned} \Psi(\dot{v}, v, \dot{q}_l, q_l) \dot{p} &= \hat{M}^1(q_l) \ddot{q}_r^1 + \hat{C}^1(q_l, \dot{q}_l) \dot{q}_r^1 \\ &\quad + \hat{G}^1(q_l), -(\hat{M}(q_l) K_\mu - \hat{C}(q_l, \dot{q}_l)) \mu \\ &\quad - \hat{M}(q_l) J^T(q_l) e_\lambda, \end{aligned} \quad (55)$$

thus,  $\theta_d$  in Eq. (30) is re-written as

$$\begin{aligned} \theta_d &= K_\sigma \sigma - \hat{K}_s^{-1} J^T(q_l) \lambda_d + \hat{M}^1(q_l) \ddot{q}_r^1 + \hat{C}^1(q_l, \dot{q}_l) \dot{q}_r^1 \\ &\quad + \hat{G}^1(q_l) - (\hat{M}(q_l) K_\mu - \hat{C}(q_l, \dot{q}_l)) \mu - \hat{M}(q_l) J^T(q_l) e_\lambda. \end{aligned} \quad (56)$$

Noting that  $\theta = \theta_d - z$  and substituting it into Eq. (10), the following closed-loop system dynamics is obtained after some manipulations on the terms in the equation

$$(K_s \widehat{M}(q_l) + I_{n-m})e_\lambda = M^1(q_l)\dot{r}^1 + C^1(q_l, \dot{q}_l)r^1 + K_s \widehat{K}_s^{-1} J^T(q_l)\lambda_d - K_s z - \beta, \quad (57)$$

where

$$\beta \triangleq (M(q_l) - K_s \widehat{M}^1(q_l))\ddot{q}_r^1 + (C(q_l, \dot{q}_l) - K_s \widehat{C}^1(q_l, \dot{q}_l))\dot{q}_r^1 + G(q_l) - K_s \widehat{G}^1(q_l) \quad (58)$$

and  $\widehat{K}_s^{-1} = K_s^{-1} - \widehat{K}_s^{-1}$ .

Multiplying both sides of Eq. (57) by  $J(q_l)M^{-1}(q_l)$  and noting that  $J(q_l)M(q_l)M^{-1}(q_l) = J(q_l)L(q_l) = 0$ , we have

$$J(q_l)M^{-1}(q_l)(K_s \widehat{M}(q_l) + I_{n-m})e_\lambda = J(q_l)M^{-1}(q_l)(C^1(q_l, \dot{q}_l)r^1 + K_s \widehat{K}_s^{-1} J^T(q_l)\lambda_d - K_s z - \beta), \quad (59)$$

$\beta$  is bounded as  $\ddot{q}_r^1 = \dot{q}_{ld}^1 + K_e \dot{e}^1$  and the other terms in Eq. (58) are bounded. With  $\beta$  and the rest terms in Eq. (59) being bounded and  $J(q_l)M^{-1}(q_l)(K_s \widehat{M}(q_l) + I_{n-m})$  being non-singular, it is concluded that  $e_\lambda$  is bounded.

Now we have shown that  $\sigma$ ,  $p - \hat{p}_s$ ,  $\mu$ ,  $\varphi_1(K_s, \widehat{K}_s^{-1})$ ,  $z$ ,  $v$ ,  $\varphi_2(\sigma, q_l, \lambda_d)$ ,  $r^1$  and  $e_\lambda$  are bounded. From the definitions of  $r^1$  and  $\sigma$  in Eqs. (16) and (17), respectively, it follows that  $r^1$ ,  $e^1$  and  $\dot{e}^1$  are all bounded. The boundedness of  $q_l(q_l^1)$ ,  $\dot{q}_l(\dot{q}_l^1)$ ,  $\lambda$  and  $\theta_d$  are guaranteed from their relations to  $e^1$ ,  $\dot{e}^1$ ,  $e_\lambda$  and planned  $q_{ld}^1$ ,  $\dot{q}_{ld}^1$  and  $\lambda_d$  which are all bounded. As  $\theta_d$  and  $z$  are bounded,  $\theta$  is bounded too. Studying Eq. (9) and multiplying both of its sides by  $L^T(q_l)$ , we have

$$M_l(q_l)\ddot{q}_l^1 = -C_l(q_l, \dot{q}_l)\dot{q}_l^1 - G_l(q_l) + L^T(q_l)K_s \theta. \quad (60)$$

Note the Property 1 is used in the above derivation.

From Property 2,  $M_l(q_l)$  is symmetric positive definite and other matrix terms in the righthand equation are bounded. As proved, the terms  $q_l^1$ ,  $\dot{q}_l^1$  and  $\theta$  are also bounded. It is obvious from Eq. (60) that  $\ddot{q}_l^1$  is bounded. It follows that  $\ddot{e}^1 = \ddot{q}_{ld}^1 - \ddot{q}_l^1$  is also bounded. Now that  $e^1$  and  $\ddot{e}^1$  are bounded, we can conclude that  $\dot{e}^1 \rightarrow 0$  when  $t \rightarrow \infty$  from Corollary 1 (Barbalat).

From Eqs. (16) and (19),  $\dot{r}^1 = \dot{q}_{ld}^1 + K_e \dot{e}^1 - \dot{q}_l^1$  which is bounded due to the boundedness of all the terms in its definition. As  $r^1$  is also bounded, we have  $r^1 \rightarrow 0$  when  $t \rightarrow \infty$  from Corollary 1 (Barbalat). From the definition of  $r^1$  in Eq. (16), it can be concluded that  $e^1 \rightarrow 0$ , or equivalently,  $q_l^1 \rightarrow q_{ld}^1$  when  $t \rightarrow \infty$ . As  $q_l$  is uniquely determined by  $q_l^1$ , it can be concluded that  $q_l \rightarrow q_{ld}$  when  $t \rightarrow \infty$ .

Summarizing what discussed in Steps 1 and 2, we have the following theorem.

**Theorem 1.** For a constrained flexible joint robotic manipulator modeled by Eqs. (1) and (2), the robot position  $q_l$  converges to its desired value  $q_{ld}$  and the force tracking error  $\lambda_d - \lambda$  is uniformly bounded if

$$\tau_m = \widehat{K}_s \theta_d + \widehat{J}_m \ddot{q}_m + k_\tau \text{sgn}(\sigma + \dot{z}), \quad (61)$$

$$k_\tau \geq \delta_K \|\theta_d\| + \delta_J \|\ddot{q}_m\|, \quad (62)$$

where

$$z = \theta_d - \theta,$$

$$\theta_d = K_\sigma \sigma - \widehat{K}_s^{-1} J^T(q_l)\lambda_d + \Psi(\dot{v}, v, \dot{q}_l, q_l)\hat{p},$$

$$\theta = q_m - q_l,$$

$$\dot{p} = \Gamma_p \Psi^T(\dot{v}, v, \dot{q}_l, q_l)\sigma,$$

$$\dot{k}_s^{-1} = -\Gamma_k \varphi_2(\sigma, q_l, \lambda_d),$$

$$\widehat{k}_s^{-1} = [k_{s1}^{-1} \ k_{s2}^{-1} \ \dots \ k_{sn}^{-1}]^T,$$

$$\widehat{K}_s^{-1} = \text{diag}[k_{si}^{-1}], \quad i = 1, 2, \dots, n,$$

$$\sigma = L(q_l)r^1 + \mu,$$

$$v = L(q_l)\dot{q}_r^1 + \mu,$$

$$\dot{\mu} + K_\mu \mu = -J^T(q_l)e_\lambda,$$

$$r^1 = \dot{e}^1 + K_e e^1,$$

$$e^1 = q_{ld}^1 - q_l^1,$$

$$e_\lambda = \lambda_d - \lambda,$$

$$\dot{q}_r^1 = \dot{q}_{ld}^1 + K_e e^1,$$

$K_\sigma > 0$ ,  $\Gamma_p > 0$  and  $\Gamma_k > 0$  are control parameters,  $\widehat{K}_s$  and  $\widehat{J}_m$  are the estimates of  $K_s$  and  $J_m$ , respectively. Regress matrix  $\Psi(\dot{v}, v, \dot{q}_l, q_l)$ ,  $\delta_K$  and  $\delta_J$  are defined in Property 4 and Assumption 2, respectively, and  $\varphi_2(\sigma, q_l, \lambda_d)$  is defined in Eq. (36).  $K_\sigma$ ,  $K_e$  and  $K_\mu$  are all positive definite control gain matrices.  $\Gamma_p$  and  $\Gamma_k$  are positive definite parameter adaptation gain matrices.

**Remark 2.** The calculation of  $\dot{z}$  in Eq. (61) is cumbersome. To avoid it, a new variable  $s_z$  is defined such that

$$s_z = \int_0^t \sigma dt + z. \quad (63)$$

Obviously

$$\text{sgn}(\sigma + \dot{z}) = \text{sgn}(\dot{s}_z) \quad (64)$$

and we only need to check the changing trend of  $s_z$  to get the sign of  $\dot{s}_z$  or  $\sigma + \dot{z}$ . In implementation, this check can be made by comparing the value of  $s_z$  in consecutive sampling times. If  $s_z$  is non-decreasing, the sign should be positive, or it should be negative.

**Remark 3.** It is well known that the sign function in the controller cause chattering problem which can be eliminated with the boundary layer approach [24]. In this approach, the sign function  $\text{sgn}(s)$  is replaced by  $s/\Delta$  when  $\|s\| < \Delta$ .  $\Delta > 0$  is defined as a boundary layer.

**Remark 4.** The measurement of joint acceleration  $\ddot{q}_m$  is required in the controller. In practice, it is not difficult to directly measure the joint acceleration. It can also be obtained by taking the difference of the joint velocity in consecutive sampling times.

**Remark 5.** Though theoretically the controller can guarantee the convergence of the link position  $q_l$  to its desired value, and the boundedness of the force tracking error  $e_\lambda$  without special requirement of the joint stiffness, a large joint stiffness (weak flexibility) increases the sensitivity of the control system to the variations of the signals in the control loops through the term  $K_s\theta$ . This may cause the system response divergent. In this case, the singular perturbation based controller [5] is more suitable.

#### 4. Simulation

The simulation example is schematically shown in Fig. 1. In this example, the end effector of a flexible joint manipulator moves along a part of the constraint surface and exerts a force on it at the same time. The length, inertia and the mass of each link of the manipulator are  $l_i = 0.3$  m,  $I_i = 0.3$  kg m<sup>2</sup> and  $m_i = 0.1$  kg, respectively ( $i = 1, 2$ ). The half of the link length is  $d_i = \frac{l_i}{2} = 0.15$  m ( $i = 1, 2$ ). The mass center of each link is assumed to be in the middle of the link.

In Fig. 1, the world coordinates is denoted by  $oxy$ . The constraint surface is described by

$$\Phi(r_d) = x_d - y_d + 0.35 = 0. \quad (65)$$

It is planned that the end effector moves along the following trajectory on the constraint surface

$$x_d(t) = -\frac{1}{10} \cos(2t),$$

$$y_d(t) = 0.35 - \frac{1}{10} \cos(2t),$$

while the magnitude of the constraint force is kept at  $\lambda_d = 2$  N.

Let the link position  $q_l = [\theta_1 \ \theta_2]^T$  and its partitions are  $q_l^1 = \theta_1$  and  $q_l^2 = \theta_2$ , respectively. The desired link positions  $q_{ld} = [\theta_{1d} \ \theta_{2d}]^T$  can be obtained from  $x_d(t)$  and  $y_d(t)$  such that

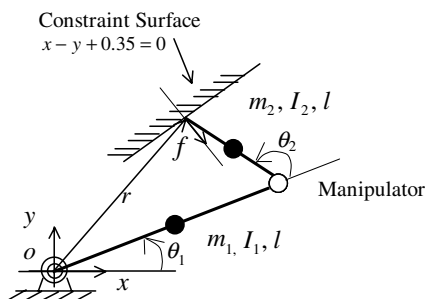


Fig. 1. Simulation example.

$$\cos(\theta_{2d}(t)) = \frac{x_d^2(t) + y_d^2(t) - d_1^2 - d_2^2}{2d_1d_2},$$

$$\sin(\theta_{2d}(t)) = -\sqrt{1 - \cos^2(\theta_{2d}(t))},$$

$$\cos(\theta_{1d}(t)) = \frac{(d_1 + d_2 \cos(\theta_{2d}(t)))x_d(t) + d_2 \sin(\theta_{2d}(t))y_d(t)}{x_d^2(t) + y_d^2(t)},$$

$$\sin(\theta_{1d}(t)) = \frac{(d_1 + d_2 \cos(\theta_{2d}(t)))y_d(t) - d_2 \sin(\theta_{2d}(t))x_d(t)}{x_d^2(t) + y_d^2(t)}.$$

Jacobians  $J(q_l)$  and  $L(q_l^1)$  are obtained as follows:

$$J(q_l) = \begin{bmatrix} -d_1 \sin(\theta_1) - d_2 \sin(\theta_1 + \theta_2) & -d_2 \sin(\theta_1 + \theta_2) \\ d_1 \cos(\theta_1) + d_2 \cos(\theta_1 + \theta_2) & d_2 \cos(\theta_1 + \theta_2) \end{bmatrix}, \quad (66)$$

$$L(q_l^1) = \left[ 1 - 1 - \frac{d_1(\sin(\theta_1) + \cos(\theta_1))}{d_2 \sin(\theta_1 + \theta_2) \cos(\theta_1 + \theta_2)} \right] \quad (67)$$

with  $J(q_l)$ , the desired link velocity  $\dot{q}_{ld}$  is obtained through  $\dot{q}_{ld} = J(q_{ld})[\dot{x}_d \ \dot{y}_d]^T$ .

Choosing the system parameter vector  $p$  as

$$p = [p_1 \ p_2 \ p_3 \ p_4 \ p_5 \ p_1 \ p_2 \ p_3 \ p_4 \ p_5],$$

where  $p_1 = I_1 + m_1 l_1^2 + I_2 + m_2(d_1^2 + l_2^2)$ ,  $p_2 = m_2 d_1 l_2$ ,  $p_3 = I_2 + m_2 l_2^2$ ,  $p_4 = (m_1 l_1 + m_2 d_1)g$ ,  $p_5 = m_2 l_2 g$  and  $g = 9.8$  m/s<sup>2</sup> is the gravitational acceleration.

The regressor matrix  $\Psi(\dot{v}, v, \dot{q}_l, q_l)$  is expressed in a required form in Eq. (13) such that

$$\Psi(\dot{v}, v, \dot{q}_l, q_l) = \begin{bmatrix} \Psi_{11} & \Psi_{12} & \Psi_{13} & \Psi_{14} & \Psi_{15} & 0 & 0 & 0 & 0 & 0 \\ 0 & 0 & 0 & 0 & 0 & \Psi_{21} & \Psi_{22} & \Psi_{23} & \Psi_{24} & \Psi_{25} \end{bmatrix},$$

where

$$\Psi_{11} = \dot{v}_1,$$

$$\Psi_{12} = 2 \cos(\theta_2) \dot{v}_1 + \cos(\theta_2) \dot{v}_2 - \sin(\theta_2) (\dot{\theta}_1 + \dot{\theta}_2) v_2 - \sin(\theta_2) \dot{\theta}_2 v_1,$$

$$\Psi_{13} = \dot{v}_2,$$

$$\Psi_{14} = \cos(\theta_1),$$

$$\Psi_{15} = \cos(\theta_1 + \theta_2),$$

$$\Psi_{21} = 0,$$

$$\Psi_{22} = \cos(\theta_2) \dot{v}_1 + \sin(\theta_2) \dot{\theta}_1 v_1,$$

$$\Psi_{23} = \dot{v}_2 + \dot{v}_1,$$

$$\Psi_{24} = 0,$$

$$\Psi_{25} = \cos(\theta_1 + \theta_2)$$

with the given physical parameters, it can be calculated that  $p_1 = 0.6135$ ,  $p_2 = 0.0045$ ,  $p_3 = 0.30225$ ,  $p_4 = 0.441$  and  $p_5 = 0.147$ . For the simulation purpose, the initial values of their estimates are set as  $\hat{p}_1(0) = 0.092$ ,  $\hat{p}_2(0) = 0.0007$ ,  $\hat{p}_3(0) = 0.045$ ,  $\hat{p}_4(0) = 0.066$  and  $\hat{p}_5(0) = 0.022$ . Assume that the robotic manipulator is initially at rest with  $q_l(0) = [2.85 \ -1.77]^T$  (rad),  $\dot{q}_l(0) = [0 \ 0]^T$  and  $\lambda(0) = 2.0$  N.

To show the effectiveness of the controller, the simulations are done for the robot with different joint flexibilities.

4.1. Simulation in the case when the joint flexibility is strong (stiffness is small)

In this case, the joint stiffness are set as  $k_{s1} = k_{s2} = 10.0$  N m. The moments of inertia of the motors are set as  $j_{m1} = j_{m2} = 0.5$  N m s<sup>2</sup>. The estimates of  $J_m$  and  $K_s$  are set to be  $\hat{K}_s = \text{diag}[8.0] \in R^{2 \times 2}$  and  $\hat{J}_m = \text{diag}[0.4] \in R^{2 \times 2}$ , respectively. The up bounds of the norms of  $\hat{K}_s$  and  $\hat{J}_m$  are thus chosen as  $\delta_K = 4$  and  $\delta_{J_1} = 2$ , respectively. The initial value of the estimate  $\hat{K}_s$  is set as  $\hat{K}_s(0) = \text{diag}[0.125] \in R^{2 \times 2}$ . The control gains and parameter adaptation gains are chosen as  $K_\sigma = \text{diag}[1.0] \in R^{2 \times 2}$ ,  $K_e = \text{diag}[3.5] \in R^{2 \times 2}$ ,  $K_\mu = \text{diag}[1.5] \in R^{2 \times 2}$ ,  $\Gamma_p = \Gamma_K = \text{diag}[0.08] \in R^{2 \times 2}$ . The width of the boundary layer is chosen to be  $\Delta = 0.002$ .

The position tracking performances of the robot and the force tracking performances are plotted in Figs. 2 and 3, respectively. The control torques for the manipulators are given in Fig. 4. The performance of parameter adaptation, represented by those of  $p_1$  to  $p_4$ , and  $k_{s1}$  to  $k_{s2}$ , are plotted in Figs. 5 and 6 respectively. It can be seen that under the proposed controller, the link positions of the robot converge to its desired values and the force tracking error is bounded. The control torques demonstrate big fluctuation at the beginning, but are within a reasonable range after some time. The parameter estimation are also stabilized and bounded. Due to the introduction of boundary layer, the chatterings in torque and force signals are smoothed out.

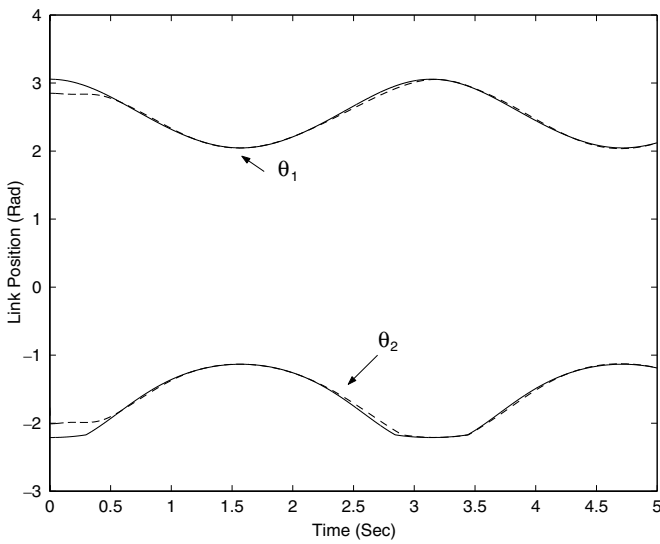


Fig. 2. Position tracking when  $K_s = \text{diag}[10.0] \in R^{2 \times 2}$  (solid: desired position, dashed: actual position).

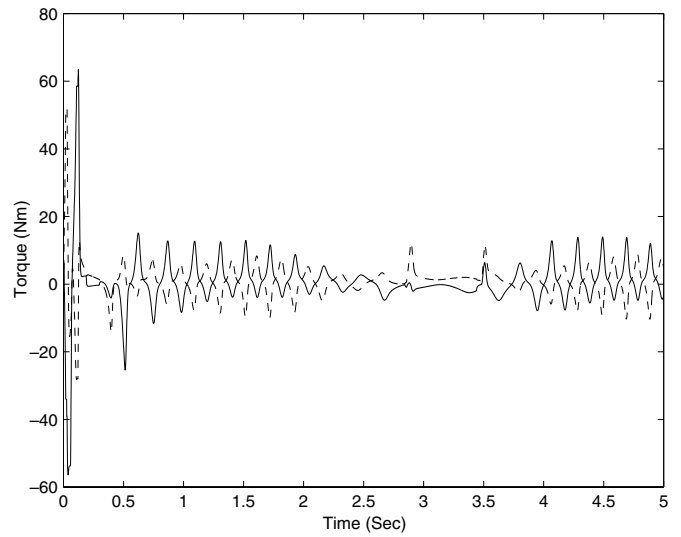


Fig. 4. Joint torques when  $K_s = \text{diag}[10.0] \in R^{2 \times 2}$  (solid: joint 1 torque, dashed: joint 2 torque).

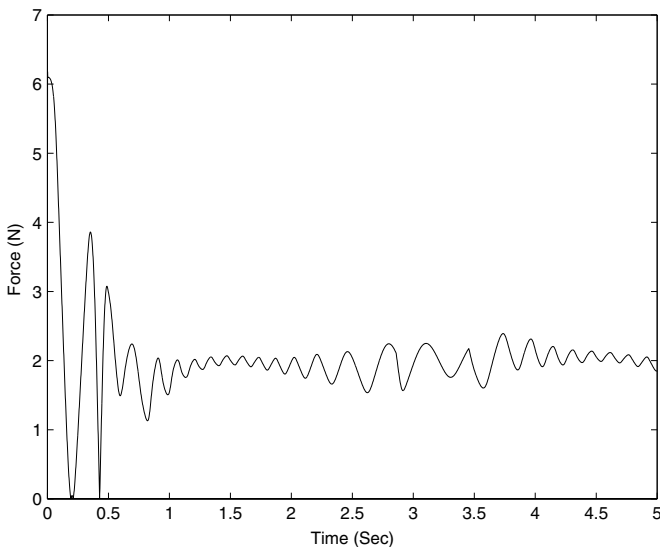


Fig. 3. Force tracking when  $K_s = \text{diag}[10.0] \in R^{2 \times 2}$  (solid: desired force, dashed: actual force).

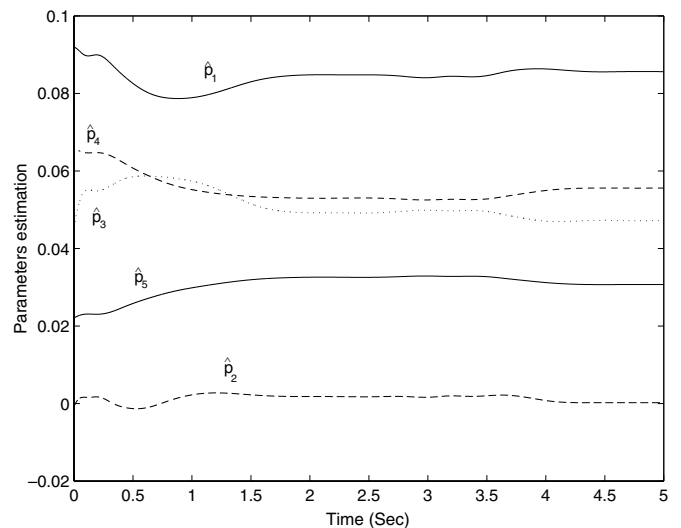


Fig. 5. Parameter estimations ( $\hat{p}_1$ ,  $\hat{p}_2$ ,  $\hat{p}_3$ ,  $\hat{p}_4$  and  $\hat{p}_5$ ) when  $K_s = \text{diag}[10.0] \in R^{2 \times 2}$ .

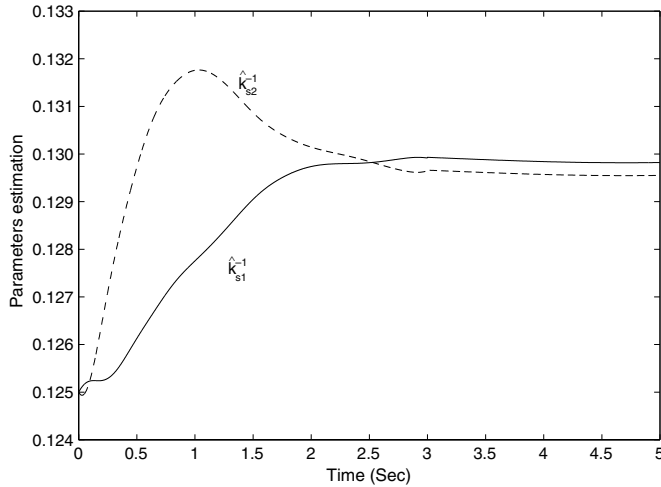


Fig. 6. Parameter estimations ( $\hat{k}_{s1}^{-1}$  and  $\hat{k}_{s2}^{-1}$ ) when  $K_s = \text{diag}[10.0] \in R^{2 \times 2}$ .

4.2. Simulation in the case when the joint flexibility is weak (stiffness is large)

In this case, the joint stiffness are set to be a bigger value:  $k_{s1} = k_{s2} = 50.0Nm$ . The initial value of the estimate  $\hat{K}_s^{-1}$  is set as  $\hat{K}_s^{-1}(0) = \text{diag}[0.02] \in R^{2 \times 2}$ . The rest parameters of the controller remain the same as in the case when the joint flexibility is strong. The simulation results are plotted from Figs. 7–11. It can be observed that though the position tracking is almost as good as that in the case when the joint flexibility is strong, the responses of the constraint force and the control inputs demonstrate bigger fluctuations and chatterings. The magnitudes of the joint torques also increase sharply. The simulation is also done for the case when  $K_s$  becomes very big (e.g.  $K_s = \text{diag}[100.0] \in R^{2 \times 2}$ ). The responses of the control system become divergent. As explained in Remark 5, in this case, the singular pertur-

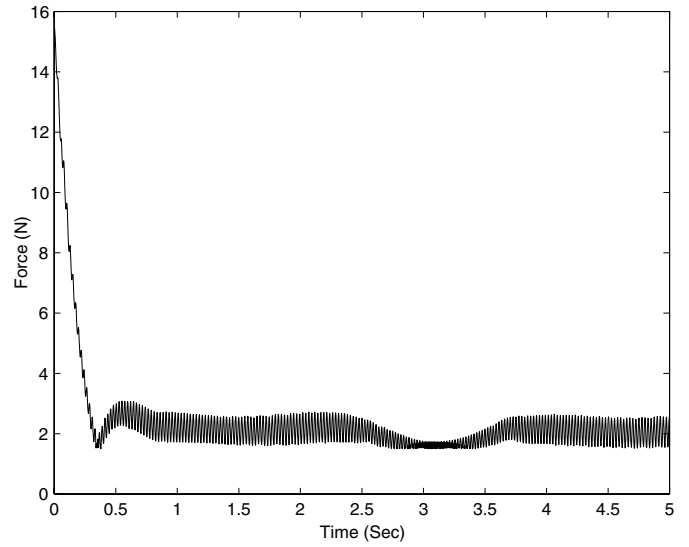


Fig. 8. Force tracking when  $K_s = \text{diag}[50.0] \in R^{2 \times 2}$  (solid: desired force, dashed: actual force).

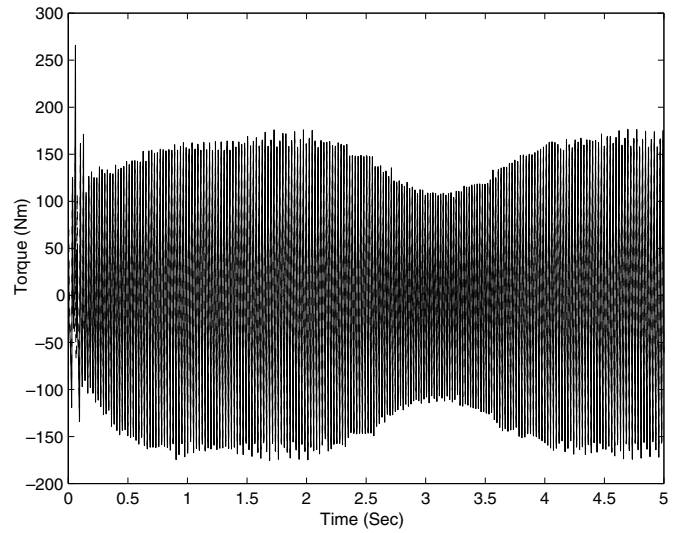


Fig. 9. Joint torques when  $K_s = \text{diag}[50.0] \in R^{2 \times 2}$  (solid: joint 1 torque, dashed: joint 2 torque).

bation based controller is more suitable, and this will be presented in a separate paper.

5. Conclusion

This paper addressed the issue of adaptive position/force control of an uncertain constrained flexible joint robots (FJR) using singular perturbation approach. The fast variables and the slow variables were defined by combing the force and position signals and the controller relied on the feedback of joint state variables (position, velocity and force) and avoided the noisy joint torque feedbacks found in many controllers developed. The proposed approach achieves the position tracking and the

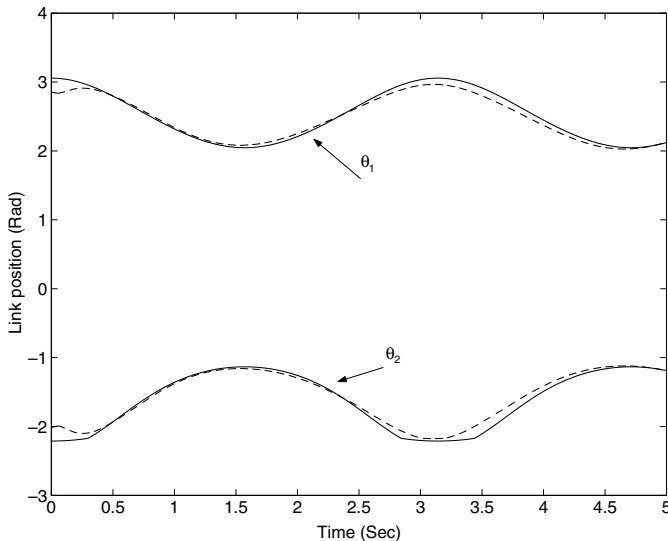


Fig. 7. Position tracking when  $K_s = \text{diag}[50.0] \in R^{2 \times 2}$  (solid: desired position, dashed: actual position).

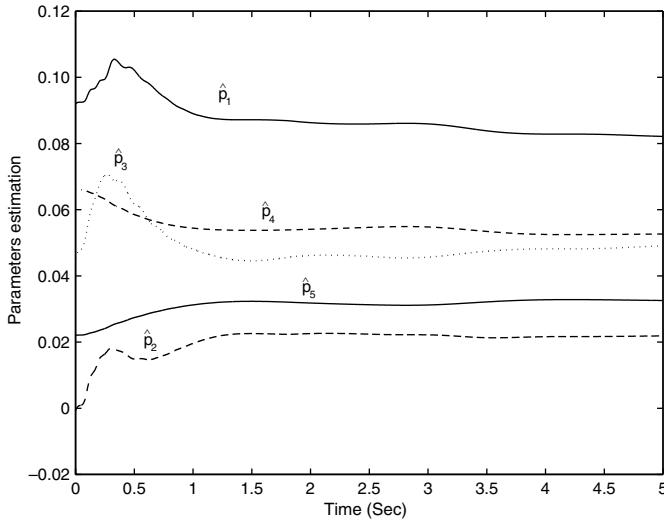


Fig. 10. Parameter estimations ( $\hat{p}_1$ ,  $\hat{p}_2$ ,  $\hat{p}_3$ ,  $\hat{p}_4$  and  $\hat{p}_5$ ) when  $K_s = \text{diag}[50.0] \in \mathbb{R}^{2 \times 2}$ .

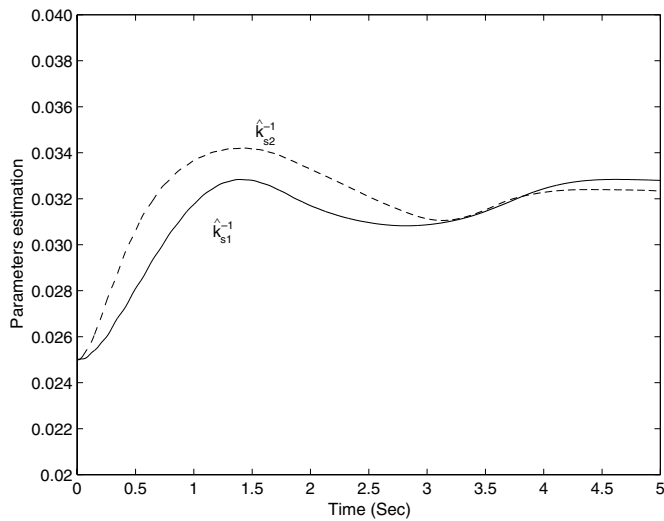


Fig. 11. Parameter estimations ( $\hat{k}_{s1}^{-1}$  and  $\hat{k}_{s2}^{-1}$ ) when  $K_s = \text{diag}[50.0] \in \mathbb{R}^{2 \times 2}$ .

boundedness of force errors for the constrained robot with weak joint flexibility (large joint stiffness).

## References

- [1] Spong MW. Modeling and control of elastic joint robots. *ASME J Dyn Syst Meas Contr* 1987;109:310–9.
- [2] Spong MW, Khorasani K, Kokotovic PV. An integral manifold approach to the feedback control of flexible joint robots. *IEEE J Robot Autom* 1987;RA-3:291–300.
- [3] Khorasani K. Adaptive control of flexible joint robots. In: *Proc IEEE int conf robot autom*, 1991. p. 2127–34.
- [4] Ge SS, Postlethwaite I. Adaptive neural network controller design for flexible joint robots using singular perturbation technique. *Trans Int MC* 1995;17(3):120–31.
- [5] Ge SS. Adaptive controller design for flexible joint manipulators. *Automatica* 1996;32(2):273–8.
- [6] Ott C, Albu-schaffer A, Hirzinger G. Comparison of adaptive and nonadaptive control laws for a flexible joint manipulator. In: *Proc 2002 IEEE/RSJ int conf on intelligent robots and systems*, 2002. p. 2018–24.
- [7] De Luca A, Isidori A, Nicolo F. Control of robot arm with elastic joints via nonlinear dynamic feedback. In: *Proc 24th IEEE conf on decision and control*, Ft. Landerdale, 1985. p. 1671–9.
- [8] Khorasani K. Nonlinear feedback control of flexible joint manipulators: a single link case study. *IEEE Trans Autom Control* 1990;35:1145–9.
- [9] Yuan J, Stepanko Y. Composite adaptive control of flexible joint robots. *Automatica* 1993;29(3):609–19.
- [10] Lozano R, Brogliato B. Adaptive control of robot manipulators with flexible joints. *IEEE Trans Autom Control* 1992;AC-37:174–81.
- [11] Brogliato B, Lozano R. Correction to adaptive control of robot manipulators with flexible joints. *IEEE Trans Autom Control* 1996;41(6).
- [12] Slotine JJE, Li WP. On the adaptive control of robot manipulators. *Int J Robot Res* 1987;6(3):49–59.
- [13] Tian L, Goldenberg AA. Robust adaptive control of flexible joint robots with joint torque feedback. In: *Proc 1995 IEEE int conf on robotics and auto*, 1995. p. 1229–34.
- [14] Oh JH, Lee JS. Control of flexible joint robot system by backstepping design approach. *Intell Autom Soft Comput* 1999;5(4):267–78.
- [15] Spong MW. On the force control problem for flexible joint manipulators. *IEEE Trans Autom Control* 1989;34(1):107–11.
- [16] Mills JK. Stability and control of elastic-joint robotic manipulators during constrained-motion tasks. *IEEE Trans Robot Autom* 1992;8(1).
- [17] Tian L, Goldenberg AA. A unified approach to motion and force control of flexible joint robots. In: *Proc 1996 IEEE int conf on robotics and auto*, 1996. p. 1115–20.
- [18] Yao B, Tomizuka M. Adaptive control of robot manipulators in constrained motion-controller design. *ASME J Dyn Syst Meas Contr* 1995;117:320–8.
- [19] Ott C, Albu-schaffer A, Kugi A, Hirzinger G. Decoupling based Cartesian impedance control of flexible joint robots. In: *Proc 2003 IEEE int conf on robotics and auto*, 2003.
- [20] Ge SS. Adaptive control of robots having both dynamical parameter uncertainties and unknown input scalings. *Mechatronics* 1996;6(5): 557–69.
- [21] McClamroch NH, Wang D. Feedback stabilization and tracking of constrained robots. *IEEE Trans Autom Control* 1988;33:419–26.
- [22] Yuan J. Adaptive control of a constrained robot—ensuring zero tracking and zero force errors. *IEEE Trans Autom Control* 1997;42(12):1709–14.
- [23] Krstic M, Kanellakopoulos I, Kokotovic P. *Nonlinear and adaptive control design*. New York: John Wiley; 1995.
- [24] Slotine JJE. Sliding controller design for nonlinear systems. *Int J Control* 1984;40(2):421–34.
- [25] Slotine JJE, Li W. *Applied nonlinear control*. Englewood Cliffs, New Jersey: Prentice Hall; 1997.